Biosensors and Bioelectronics 54 (2014) 408–414

Contents lists available at ScienceDirect

Biosensors and Bioelectronics

journal homepage: www.elsevier.com/locate/bios

Signal amplification for thrombin impedimetric aptasensor: Sandwich protocol and use of gold-streptavidin nanoparticles ☆

Cristina Ocaña, Manel del Valle *

Sensors and Biosensors Group, Department of Chemistry, Universitat Autonoma de Barcelona, 08193 Bellaterra, Spain

ARTICLE INFO

Article history:
Received 26 July 2013
Received in revised form
4 October 2013
Accepted 21 October 2013
Available online 7 November 2013

Keywords:
Impedance
Nanoparticles
Aptamer
Biosensor
Thrombin
Quantum dots

ABSTRACT

In this work, we report a highly specific amplification strategy demonstrated for the ultrasensitive biosensing of thrombin with the use of gold-streptavidin nanoparticles (strep-AuNPs) and silver reduction enhancement. The biotinylated aptamer of thrombin was immobilized onto an avidin-graphite epoxy composite (AvGEC) electrode surface by affinity interaction between biotin and avidin; electrochemical impedance measurements were performed in a solution containing the redox marker ferrocyanide/ferricyanide. The change in interfacial charge transfer resistance (R_{ct}) experimented by the redox marker, was recorded to confirm aptamer complex formation with target protein, thrombin (Thr), in a label-free first stage. A biotinylated second thrombin aptamer, with complementary recognition properties was then used in a sandwich approach. The addition of strep-AuNPs and silver enhancement treatment led to a further increment of R_{ct} thus obtaining significant signal amplification. The AptThrBio1-Thr-AptThrBio2 sandwich formation was inspected by confocal microcopy after incubation with streptavidin quantum dots. In order to visualize the presence of gold nanoparticles, the same silver enhancement treatment was applied to electrodes already modified with the nanoparticle-sandwich conjugate, allowing direct observation by scanning electron microscopy (SEM). Results showed high sensitivity and selectivity for thrombin detection, with an improvement from ca. 4.7 pM in a simple assay to 0.3 pM in the amplified reported scheme.

1. Introduction

Aptamers are synthetic nucleic acids (DNA or RNA) which selectively bind to low-molecular-weight organic or inorganic substrates or to macromolecules such as proteins (Jayasena, 1999). The affinity constant of aptamers toward their substrates lies in the micromolar to nanomolar range, comparable to the binding constants of antibodies to antigens (Jenison et al., 1994). The interest in aptamers as specific binding agents originates from the relative ease of their preparation by an evolutionary selection procedure that eliminates the need for sophisticated design of the receptor units. Not surprisingly, aptamers have found growing interest as active separation materials in chromatography (Kotia et al., 2000), and electrophoresis (Clark and Remcho, 2002), as therapeutic (Biesecker et al., 1999; Hicke et al., 2001) or diagnostic agents, and as active materials for biosensing (Evtugyn et al., 2012). The use of aptamers for biosensing is particulary interesting, as aptamers could substitute antibodies in bioanalytical sensing given they reveal obvious advantages over immunosensors. The aptamer of thrombin is the most known and utilized aptamer. Thrombin is the last enzyme protease involved in the coagulation cascade, and converts fibrinogen to insoluble fibrin which forms the fibrin gel, both in physiological conditions and in a pathological thrombus (Holland et al., 2000). Therefore, thrombin plays a central role in a number of cardiovascular diseases (Burgering et al., 1997), and is thought to regulate many processes such as inflammation and tissue repair at the blood vessel wall. Concentration levels of thrombin in blood are very low, and levels down to the picomolar range are associated with disease; because of this, it is important to assess its concentration at trace level (Centi et al., 2007).

In recent years, there has been large interest in the development of aptasensors. Aptasensors are biosensors that use aptamers as the biorecognition element. This type of biosensors can be classified, depending on the technique employed for transduction, into optical (Lee and Walt, 2000), piezoelectric (Srijanto et al., 2012) and electrochemical types (Ocaña et al., 2012; Radi et al., 2005). Electrochemical aptasensors make use of electrochemical transduction for biosensing. Recently, among the different electrochemical techniques available, electrochemical impedance spectroscopy (EIS) (McDonald, 1987), has been used in numerous studies, also for protein detection (Lisdat and Schafer, 2008; Radi et al., 2005). This technique is very sensitive to changes in the

☆This work was presented as Poster P126 at the 3rd International Conference on Bio-Sensing Technology 2013 (BITE 2013), held in Sitges (Barcelona) on 12–15 May 2013.

* Corresponding author. Tel.: +34 935813235; fax: +34 935812477.
E-mail addresses: manel.delvalle@uab.cat, manel.delvalle@uab.es (M. del Valle).

0956-5663/$ - see front matter © 2013 Elsevier B.V. All rights reserved.
http://dx.doi.org/10.1016/j.bios.2013.10.068

interfacial properties of the modified electrodes caused by biorecognition events at the electrode surface (Bardea et al., 1999; Loo et al., 2012). For this reason, EIS is becoming an attractive electrochemical technique for numerous applications such as immunosensing (Loo et al., 2012), genosensing (Bonanni et al., 2010), enzyme activity determinations (Li et al., 2012), studies of corrosion (Blin et al., 2007) or other surface phenomena (Liao et al., 2007).

Gold nanoparticles have been widely used in biosensing for tagging purposes and also for amplification thanks to their excellent properties, such as high biocompatibility, distinctive size-related electronic and optical behavior, high electrical conductivity and high catalytic activity. In recent years, several protocols using gold nanoparticles-assisted electrochemical aptamer biosensing were developed with the aim of enhancing the electrochemical response (Deng et al., 2008; Zheng et al., 2007).

In this work, we report a highly specific amplification strategy demonstrated for the ultrasensitive detection of thrombin with the use of streptavidin gold nanoparticles and silver enhancement treatment. The transducer employed consisted of an avidin graphite-epoxy composite electrode (AvGEC), of general use in our laboratories and already extensively studied and applied to amperometric, enzymatic, immuno and genosensing assays (Bonanni et al., 2006; Merkoci et al., 2005; Pumera et al., 2005). The uneven surface of the avidin graphite-epoxy electrode allows the immobilization of biotinylated aptamer of thrombin (AptThrBio1) on its surface by affinity interaction between biotin and avidin. The change of interfacial charge transfer resistance (R_{ct}) experimented by the redox marker was recorded to confirm the aptamer sandwich formation with target protein, thrombin (Thr). Then, a biotinylated second thrombin aptamer (AptThrBio2), with complementary recognition properties to those used in the previous approach was employed to form the sandwich. The addition of strep-AuNPs and silver enhancement treatment led to a further increment of R_{ct} and the subsequent achievement of significant signal amplification, high sensitivity and improvement of selectivity.

2. Experimental

2.1. Chemicals

Potassium dihydrogen phosphate, potassium ferricyanide $K_3[Fe(CN)_6]$, potassium ferrocyanide $K_4[Fe(CN)_6]$, sodium monophosphate, streptavidin gold nanoparticles, 655 nm streptavidin quantum dots (strep-QDs), avidin and the target protein thrombin (Thr), were purchased from Sigma (St. Louis, MO, USA). Poly (ethylene glycol) 1000 (PEG), sodium chloride and potassium chloride were purchased from Fluka (Buchs, Switzerland). LI silver enhancement kit was obtained from Nanoprobes (Yaphank, New York). All-solid-state electrodes (AvGECs) were prepared using 50 μm particle size graphite powder (Merck, Darmstadt, Germany), Epotek H77 resin and its corresponding hardener (both from Epoxy Technology, Billerica, MA, USA), and avidin. All reagents were analytical reagent grade. Aptamers used in this study were purchased from TIB-MOLBIOL (Berlin, Germany). Stock solutions of aptamers were diluted with sterilized and deionised water, separated into fractions and stored at −20 °C until required. Their base sequences were:

- AptThrBio1: 5′-GGTTGGTGTGGTTGG-Biotin-3′,
- AptThrBio2: 5′-Biotin-AGTCCGTGGTAGGGCAGGTT GGGGTGACT-3′ and
- AptCytc: 5′-Biotin-AGTGTGAAATATCTAAAC TAAATGTGGAGGGTGGGACGGGAAGAAGTTTATTTTTCACACT-3′.

All solutions were made up using MilliQ water from MilliQ System (Millipore, Billerica, MA, USA). The buffers employed were: PBS (187 mM NaCl, 2.7 mM KCl, 8.1 mM $Na_2HPO_4 \cdot 2H_2O$, 1.76 mM KH_2PO_4, and pH 7.0) and 10 nM PBS without NaCl and KCl.

2.2. Apparatus

AC impedance measurements and cyclic voltammetry were performed with the aid of an Autolab PGStat 20 (Metrohm Autolab B.V, Utrecht, The Netherlands). FRA and GPES (Metrohm Autolab) software were used for data acquisition and control of the experiments. A three electrode configuration was used to perform the impedance and cyclic voltammetry measurements: a platinum-ring auxiliary electrode (Crison 52-67 1, Barcelona, Spain), a Ag/AgCl reference electrode and the constructed AvGEC as the working electrode (with a geometric area of 0.28 cm^2). Temperature-controlled incubations were done using an Eppendorf Thermomixer 5436. A scanning electron microscope (SEM) (Merlin, Zeiss, Germany) and a confocal microscope (SP5, Leica, Solms, Germany) were used to visualize the silver enhanced strep-AuNPs and strep-QDs respectively on the electrode surface.

2.3. Construction of working electrodes

The electrodes were prepared using a PVC tube body (6 mm i.d.) and a small copper disk soldered to the end of an electrical connector. The conductive part of AvGECs was an avidin epoxy graphite conductive paste, formed from graphite (18%), avidin (2%) and epoxy resin (80%), which was deposited into the cavity in the plastic body, filling it, as shown Fig. 1(a) (Bonanni et al., 2007). The composite material was cured in an oven at 40 °C for 7 days. Before each use, the electrode surface was moistened with MilliQ

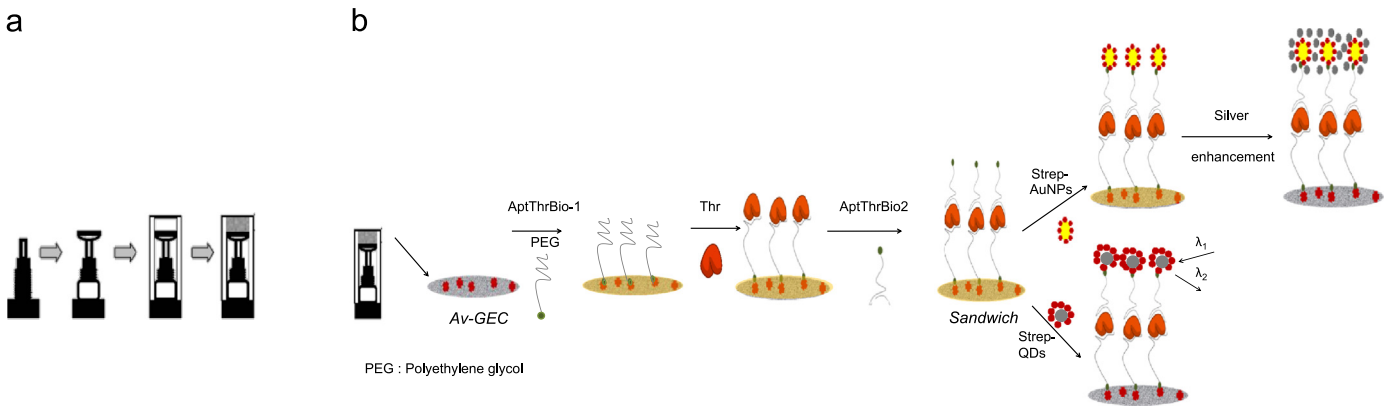

Fig. 1. (a) Scheme of construction of avidin graphite-epoxy composite electrodes and (b) scheme of the biosensing procedure.

water and then thoroughly smoothed with abrasive sandpaper and finally with alumina paper (polishing strips 301044-001, Orion) in order to obtain a reproducible electrochemical surface (Lermo et al., 2007; Williams et al., 2003).

2.4. Protein capture and amplification protocol

The scheme of experimental protocol for thrombin analysis, described in detail below, is represented in Fig. 1(b).

2.4.1. Aptamer immobilization

The first step consists of aptamer AptThrBio1 immobilization on the electrode surface. A volume of 160 μL of MilliQ water containing 35 pmol of aptamer solution was heated to 80–90 °C for 3 min to promote the loose conformation of the aptamer. Then, the solution was dipped in a bath of cold water and the electrode was immersed in it, where the avidin–biotin affinity interaction took place for 15 min at the electrode surface. This was followed by two washing steps using PBS buffer solution for 10 min, in order to remove any unadsorbed aptamer.

2.4.2. Blocking step

To minimize any possible nonspecific adsorption, the electrodes were dipped in 160 μL of PEG 40 mM. This was followed by two washing steps using PBS buffer solution for 10 min.

2.4.3. Thrombin detection

The electrodes were dipped in a solution with the desired concentration of Thr. The incubation took place for 15 min. Then, the biosensors were washed twice with PBS buffer solution for 10 min.

2.4.4. Sandwich formation

In order to achieve the aptamer sandwich formation, the electrodes were dipped in 160 μL of PBS solution containing 12 pmol of AptThrBio2. The incubation took place for 15 min. This was followed by two washing steps using PBS buffer solution for 10 min.

2.5. Amplification

Two different variants were used, with employ of quantum dots, just for visualizing the sandwich formed, and with employ of strep-AuNPs for impedimetric signal amplification.

2.5.1. Addition of strep-QDs

Av-GEC electrodes modified with the biotin end aptamer sandwich were incubated in a solution of 40 nM of strep-QDs for 20 min at 25 °C with stirring. Then the electrodes were washed twice with 10 mM PBS buffer. Negative controls were performed for the strep-QDs addition step either using AptCytc as second aptamer.

2.5.2. Addition of strep-AuNPs

Av-GEC electrodes modified with the sandwich complex were incubated in 160 μL of strep-AuNPs, from a 1/100 dilution of the stock solution in PBS buffer. The tube was incubated at 25 °C with gentle stirring for 20 min. This step was followed by two gentle washing steps in PBS buffer for 10 min at 25 °C. Negative controls were performed for the strep-AuNPs addition step using AptCytc as aptamer without affinity.

2.5.3. Silver enhancement of strep-AuNPs

Twenty microliters of a solution obtained by the combination of 10 μL of enhancer and 10 μL of initiator were deposited onto the electrode surface and left for 7 min to facilitate the reaction. Silver enhancement occurs during the catalytic reduction of silver from one solution (e.g. the enhancer) by another (e.g. the initiator) in the presence of gold particles. The reduction reaction causes silver to build up on the surface of the gold nanoparticles. After this catalytic silver reduction, the electrodes were thoroughly washed with deionized water to stop the reaction. The silver enhancing solution was prepared immediately before each use. For silver enhancement treatment, the negative control used was a non-biotinylated AptCytc as aptamer without affinity.

Different selectivity experiments carried out were performed with the same protocol unless were specified.

All incubations were carried out at controlled temperature in the thermomixer.

2.6. Impedimetric detection

Impedance experiments were carried out at an applied potential of 0.17 V (vs. Ag/AgCl reference electrode), with a range of frequency of 50 KHz–0.05 Hz, an AC amplitude of 10 mV and a sampling rate of 10 points per decade above 66 Hz and 5 points per decade at the lower range. All measurements were performed in PBS buffer containing 0.01 M $K_3[Fe(CN)_6]/K_4[Fe(CN)_6]$ (1:1) mixture, used as a redox marker. The impedance spectra were plotted in the form of complex plane diagrams (Nyquist plots, $-Z_i$ vs. Z_r) and fitted to a theoretical curve corresponding to the equivalent circuit with Z_{view} software (Scribner Associates Inc., USA). The equivalent circuit was formed by one resistor/capacitor element in series with a resistance. In it, the resistance in series with the capacitor element, R_1, corresponds to the resistance of the solution, the resistance in parallel with the capacitor element, R_{ct}, is the charge transfer resistance between the solution and the electrode surface, whilst the capacitor element is the constant phase element (CPE) associated with the double-layer capacitance. The use of a CPE instead of a capacitor is required to optimize the fit to the experimental data, and this is due to the nonideal nature of the electrode surface. For all performed fittings, the chi-square goodness-of-fit test was thoroughly checked to verify calculations. In all cases, calculated values for each circuit remained in the range of 0.0003–0.15 much lower than the tabulated value for 50 degrees of freedom (67.505 at 95% confidence level). In this work, we focused on the variation of charge resistance transfer (R_{ct}), as indicator of changes on the electrode surface. In order to compare the results obtained from the different electrodes used, and to obtain independent and reproducible results, a relative transformation of signals was needed (Bonanni et al., 2006). Thus, the Δ_{ratio} value was defined according to the following equations:

$$\Delta_{ratio} = \Delta_s / \Delta_p$$

$$\Delta_s = R_{ct\ (AptThrBio1\text{-}Thr/AptThrBio2/strep\text{-}AuNPs/silver\ enhancement)} - R_{ct\ (electrode\text{–}buffer)}$$

$$\Delta_p = R_{ct\ (AptThrBio1)} - R_{ct\ (electrode\text{–}buffer)}$$

where $R_{ct\ (AptThrBio1\text{-}Thr/AptThrBio2/strep\text{-}AuNPs/silver\ enhancement)}$ was the electron transfer resistance value measured after aptamer sandwich formation; $R_{ct\ (AptThrBio1)}$ was the electron transfer resistance value measured after aptamer immobilization on the electrode, and $R_{ct\ (electrode\text{–}buffer)}$ was the electron transfer resistance of the blank electrode and buffer.

3. Results

3.1. Electrode surface area characterization

Effective surface area was characterized by CV using a known procedure (Shi et al., 2011). CVs for bare electrodes in ferricyanide

followed expected trends, and a plot of peak current vs. the square root of scan rate was linear, (see Supplementary information, Fig. S2). Using the Randles–Sevcik equation (Bard and Faulkner, 2000), the effective surface area of AvGEC was $0.197 \pm 0.05\ cm^2$, while its geometric area was $0.28\ cm^2$. The avidin protein present in the composite decreased the effective area due to the protein insulating nature, thus decreasing the effective surface area available for signal transduction. This observation is also in agreement with impedance characterization of bare electrodes, just the epoxy-graphite composite vs. those modified with avidin, whereas the latter present increased impedance, in the form of larger R_{ct}.

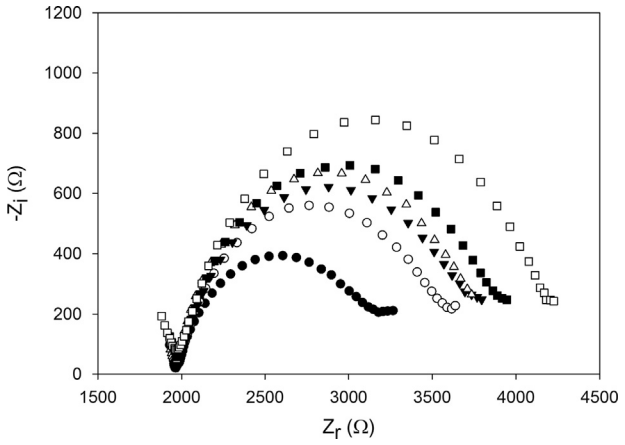

Fig. 2. Nyquist diagrams for EIS measurements of: •, bare AvGEC electrode; ○, biotinylated aptamer of thrombin 1; ▾, biotinylated aptamer of thrombin and thrombin protein; △, sandwich complex; ■, sandwich complex modified with strep-AuNPs; and □, sandwich complex modified with strep-AuNPs and silver enhancement treatment. All experiments were performed in PBS solution and all EIS measurements were performed in PBS solution containing 0.01 M $K_3[Fe(CN)_6]$/$K_4[Fe(CN)_6]$.

3.2. EIS characterization

For the operation details of the proposed aptasensor, the amounts used of AptThrBio1 and PEG were optimized in a previous work (Ocaña et al., in press); the AptThrBio2 amount used was optimized by building its titer curve (see Supplementary information, Fig. S1), and the strep-AuNPs were used just in excess to AptThrBio2.

In Fig. 2, the EIS spectrum obtained for a biosensing experiment using aptamer sandwich protocol and silver enhancement amplification are shown. Impedance measurements were performed before modifying the electrode surface (bare Av-GEC electrode), after modifying the electrode surface with AptThrBio1, Thr, AptThrBio2 (sandwich formation), strep-AuNPs and finally, after silver deposition. As shown in this figure, R_{ct} increased after any modification of the electrode surface. This can be due to the increased difficulty of the redox reaction of $[Fe(CN)_6]^{3-/4-}$ to take place, due to the sensor surface alteration (Katz and Willner, 2003). Two different factors may be taken into account to explain this: the electrostatic repulsion and the sterical hindrance. The former is more significant in the first step of protocol; when the AptThrBio1 is immobilized onto the electrode surface by avidin–biotin affinity, a first layer is formed, where negatively charged phosphate groups of aptamer skeleton are responsible of the electrostatic repulsion of the negatively charged redox marker, thus inhibiting the interfacial transfer process and resulting in R_{ct} increment. The addition of Thr and a second ApThrBio2 to form a

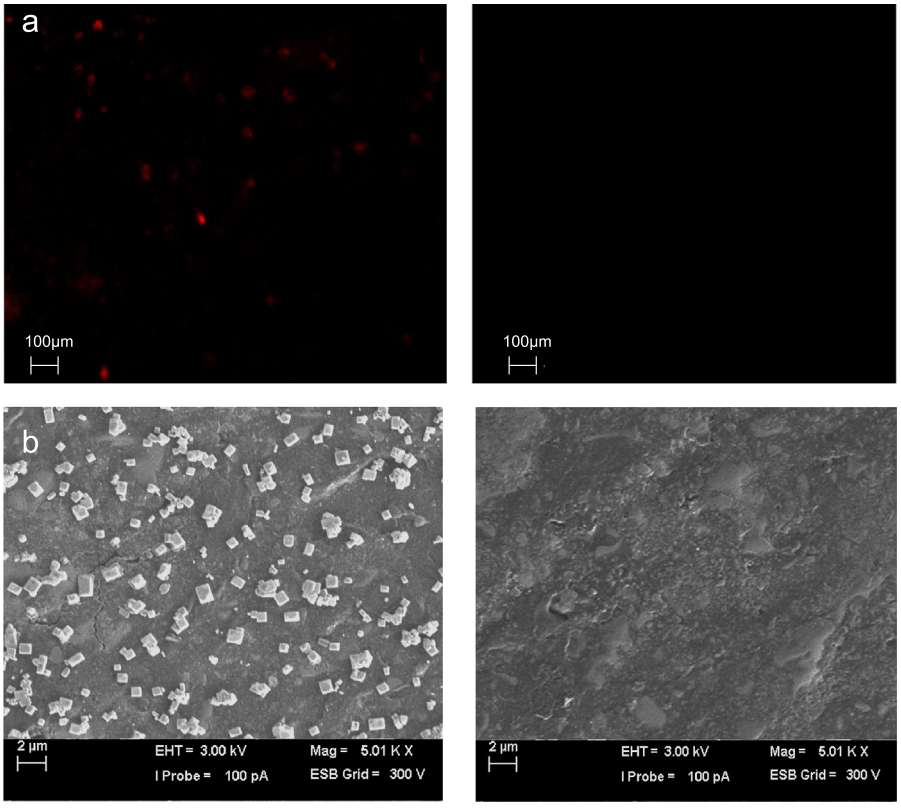

Fig. 3. (a) Confocal images of: (left) positive control using biotinylated aptamer of thrombin 1+thrombin+biotinylated aptamer of thrombin 2+strep-QDs and (right) negative control using biotinylated aptamer of thrombin 1+thrombin+biotinylated aptamer of cytochrome c+strep-QDs. (b) SEM images of: (left) experiment using biotinylated aptamer of thrombin 1+thrombin+biotinylated aptamer of thrombin 2+strep-AuNPs+silver enhancement treatment and (right) negative control using biotinylated aptamer of thrombin 1+thrombin+biotinylated aptamer of cytochrome c+strep-AuNPs+silver enhancement treatment. SEM images were taken at a acceleration voltage of 3 KV and a resolution of 2 µm and confocal images were collected at 625 nm and with excitation wavelength of 405 nm.

sandwich results in a further increment of R_{ct} due to the increased quantity of negative charge and the hindrance caused by the formation of a double layer. In this work, strep-AuNPs and silver enhancement treatment were used with the aim of amplifying the EIS sandwich formation signal. After the addition of strep-AuNPs we can observe an increment of R_{ct} value because of the increased space resistance due to Au-streptavidin conjugates. Working at pH 7, streptavidin is slightly negatively charged (pI is around pH 5) and this fact also contributes to enhancement of impedance (Sivasankar et al., 1998). In the second amplification step, silver enhancement treatment (Cai et al., 2002; Hanaee et al., 2007), a significant increment of R_{ct} value was also observed and attributable to the silver deposition on gold.

3.3. Confocal microscopy characterization

Aptamer sandwich formation was inspected by confocal microscopy after incubation with the strep-QDs. The images obtained are shown in Fig. 3(a). The first image (Fig. 3(a), left) corresponds to the electrodes modified with aptamer sandwich formation and strep-QDs. The fluorescence points observed in this case are due to the presence of the complex formed between strep-QDs and the aptamer sandwich conjugated through the biotin–streptavidin affinity. The weak fluorescence observed in the second image (Fig. 3(a) right) corresponds to the negative control, which did not use biotinylated complementary aptamer. Comparison of the two images indicates that AptThrBio2 recognizes Thr and forms the expected sandwich conjugate.

3.4. Scanning electron microscope characterization

In order to visualize the presence and distribution of gold nanoparticles, the silver enhancement treatment was used. These experiments also provided an image of the homogeneity and accessibility of the anchorage points supplied by the avidin entrapped in the biocomposite. SEM images taken at an acceleration voltage of 3 kV are shown in Fig. 3(b) left, illustrating a positive experiment with aptamer sandwich and strep-AuNPs. As it can be observed in Fig. 3(b) left, the distribution of silver enhanced-gold nanoparticles is quite homogeneous. This also implies a regular distribution of avidin molecules in the biocomposite and well-organized formation of aptamer sandwich onto the electrode surface. Apart, the nanoparticles formed were monocrystalline; that is, thanks to the disposition of the streptavidin around of gold nanoparticles, the silver crystallized in specific directions. Comparing this experiment with the negative control that did not use the biotinylated complementary aptamer, Fig. 3(b) right, a surface without nanoparticles can be observed.

3.5. Analytical performance of the aptasensor for detection of thrombin

Taking the already established reaction conditions for AptThrBio1, AptThrBio2 and PEG, the proposed aptasensor was then used following the sandwich protocol, plus amplification employing the strep-AuNPs and silver enhancement treatment. Fig. 4(a) shows calibration curves with increasing concentrations of Thr and Fig. 4(b), their respective regression curves in the linear range, at the different steps of the protocol: (1) AptThrBio1-Thr, (2) sandwich formation between AptThrBio1, Thr and AptThrBio2, (3) aptamer sandwich modified with strep-AuNPs, and (4) aptamer sandwich modified with strep-AuNPs and silver enhancement treatment. In our previous experience with silver enhancement, related to DNA hybridization biosensing, it was not possible to obtain good impedimetric measurements following amplification treatment (Bonanni et al., 2008). In this case, although the reproducibility was not excellent, the calibration curve obtained showed a good RSD. As can be seen in Fig. 4(a), all calibration curves increased until the value of 100 pM of Thr, this could be due to the fact that concentrations larger than 100 pM cause a saturation on the sensor surface. Moreover, a signal increment of up to 89% between AptThrBio1-Thr (the simple biosensing) and sandwich formation with strep-AuNPs and silver enhancement treatment was observed. As can be observed in Table 1, the use of silver enhancement treatment led to the highest sensitivity and signal amplification compared to the other calibration curves obtained. This confirms that the silver deposition on gold nanoparticles increases essentially the sterical hindrance, producing an increment of observed impedance. Despite a higher sensitivity, the detection limit obtained in this case, 0.3 pM, is slightly worse than the one obtained with only strep-AuNPs. This fact, caused by the deteriorated reproducibility, could be attributable to the increased number of process steps and associated increased potential errors. The best detection limit, approximately 0.2 pM, corresponded to the sandwich and strep-AuNPS calibration curve. This confirmed that the proposed methods may reach a low detection limit and ultrahigh sensitivity for the detection of thrombin.

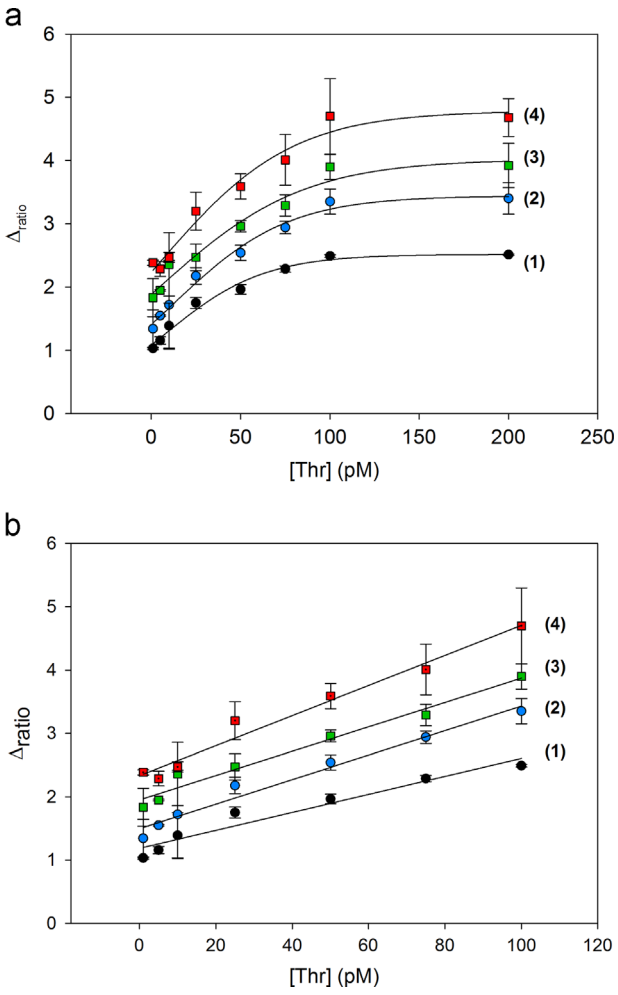

Fig. 4. (a) Calibration curves and (b) linear portions of: (1, black circle) biotinylated aptamer of thrombin 1, (2, blue circle) sandwich complex, (3, green square) sandwich complex modified with strep-AuNPs, and (4, red square) sandwich complex modified with strep-AuNPs and silver enhancement treatment. All experiments were performed in PBS solution and all EIS measurements were performed in PBS solution containing 0.01 M $K_3[Fe(CN)_6]/K_4[Fe(CN)_6]$. Uncertainty values corresponding to replicated experiments ($n=5$). (For interpretation of the references to color in this figure legend, the reader is referred to the web version of this article.)

Table 1
Summary of calibration results.

Calibration curve	*Regression curve*	*Detection limit* (pM)	*Linear range* (pM)	*% RSD*[a]	*% Amplification*
AptThrBio1-Thr	$\Delta_{ratio}=1.042+0.0157[Thr]$	4.7	0.75–100	2.2	–
Aptamer sandwich	$\Delta_{ratio}=1.495+0.0194[Thr]$	2	0.75–100	3.4	35
Aptamer sandwich/strep-AuNPs	$\Delta_{ratio}=1.874+0.0201[Thr]$	0.2	0.1–100	5.2	57
Aptamer sandwich/strep-AuNPs/silv.enh	$\Delta_{ratio}=2.477+0.0219[Thr]$	0.3	0.1–100	9.9	89

[a] Corresponding to five replicate experiments at 75 pM thrombin.

Table 2
Comparison of proposed biosensor with other reported methodologies for thrombin detection.

Analytical technique	Detection limit	Reference
Amperometry	0.12 pM	Bai et al. (2013)
Potentiometry	6.7 nM	Goda and Miyahara (2013)
Voltammetry	0.52 pM	Fu et al. (2013)
DPV	7.82 aM	Zheng et al. (2007)
EIS	4.4 pM	Xu et al. (2013)
EIS	0.1 pM	Deng et al. (2008)
EIS and CV	93 pM	Zhang et al. (2013)
EIS	0.2 pM	Our work
SPR	0.1 nM	Bai et al. (2013)
Electroluminiscence	1.6 fM	Gui et al. (2013)
Electroluminiscence	0.4 pM	Wang et al. (2013)
Electroluminiscence	0.5 pM	Yang et al. (2013)
SERS	0.16 pM	Wu et al. (2013)
PET	13 pM	Zhang et al. (2013)
FRET	2.5 nM	Chen et al. (2013)
Fluorescence	1.1 nM	Kong et al. (2013)

When the proposed aptasensor was compared with other detection methodologies for thrombin detection, some interesting facts are inferred. The results are shown in Table 2, where sensitivity information is presented as the LOD of each biosensor compared. The lowest detection limit value among all the analytical techniques corresponded to (Zheng et al., 2007), but this Thr biosensor used a double amplification strategy, with thiocyanuric acid and gold nanoparticle-labeled aptamer, and differential pulse voltammetry (DPV). Our proposed aptasensor is on the second range of lowest LOD in electrochemical techniques and impedance, thus demonstrating satisfactory results for the detection of thrombin in real samples, given that this level corresponds to physiological concentration. Moreover, the proposed aptasensor showed many advantages: it is stable for 7 days, its surface is easily regenerable by polishing and the followed procedure was simple and easy.

3.6. Selectivity of the aptasensor

To verify that the signal was dependent on the specific recognition, our protocol for thrombin detection was evaluated by challenging it with possible interfering proteins present in blood serum, comparing it to the simple biosensing, label-free detection alternative, see Fig. 5. From this investigation, we found that the presence of interfering proteins such as albumin, cytochrome c, fibrinogen, prothrombin and immunoglobulin G, at serum concentration level exhibits negligible response compared with 75 pM Thr in the amplified sandwich protocol, even at concentrations four or five orders of magnitude higher than typical Thr concentration. The figure also demonstrates that the sandwich protocol displays a clear advantage, more than the signal amplification, the marked decrease of interfering effects that are still noticeable in the simple biosensing scheme. These observations suggest that the sensing mechanism relies on specific recognition and that the aptasensor sandwich method is highly specific for the

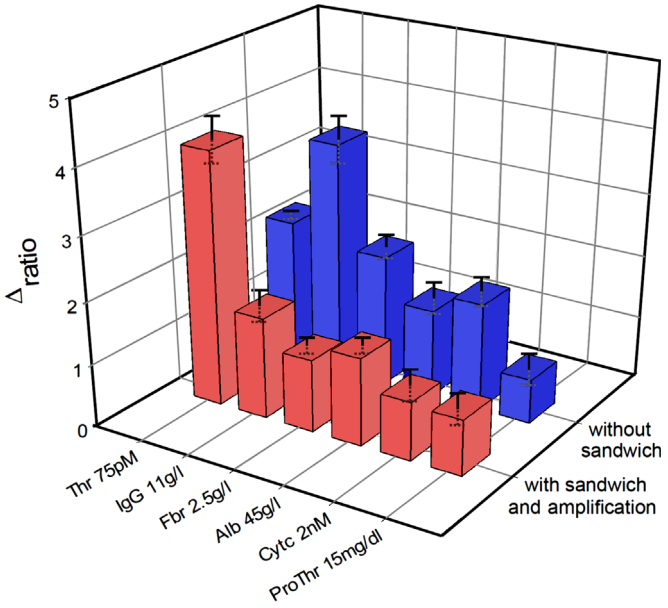

Fig. 5. 3D bar chart of response towards different proteins present in serum, without the amplification protocol and with the sandwich/amplification protocol. Uncertainty values corresponding to replicated experiments ($n=5$).

detection of Thr. Moreover, it is important to emphasize that prothrombin protein is the precursor of thrombin in the blood clotting process and this aptasensor is capable of distinguishing both proteins with high selectivity.

Apart of these proteins, other common compounds present in blood were also tested for interference (see Supplementary information Fig. S3). Uric and ascorbic acid showed negligible responses compared with 75 pM Thr, tested at concentrations eight and six orders of magnitude higher than that of Thr. Dopamine exhibited certain low interfering signal (17%) at typical serum concentration, but it should be considered that this compound is only present in serum during physical and emotional stress.

4. Conclusions

In this work, the impedimetric signal amplification for the detection of thrombin was proposed using an aptamer sandwich formation with strep-AuNPs and silver enhancement treatment. The use of strep-AuNPs and strep-QDs permitted rapid formation of an easily detected conjugate with a biotinylated aptamer sandwich through a streptavidin–biotin interaction. Thanks to the signal amplification with strep-AuNPs and silver deposition, it was possible to increase the sensitivity of the method. Besides, for a comparable amount of AptThrBio1-Thr, the signal resulted in 89% amplification, compared to results recorded with simple biosensing AptThrBio1-Thr. Moreover, the limit of detection obtained was 0.3 pM. A good linear range, 0.1–100 pM, and high

selectivity with respect to different serum proteins and organic compounds at serum concentration level were also attained with this protocol. The silver enhancement treatment also permitted to visualize the gold nanoparticles on the electrode surface with SEM. This allowed confirming the proposed steps of the protocol and a homogeneous distribution of biosensing sites on the electrodes. We believe that this method could be extended for the determination of other proteins in serum and that it results promising for clinical application.

Acknowledgments

Financial support for this work has been provided by Spanish Ministry of Science and Innovation, (MICINN, Madrid) through Project CTQ2010-17099 and by the Catalonia program ICREA Academia. Cristina Ocaña thanks the support of Ministry of Science and Innovation (MICINN, Madrid, Spain) for the predoctoral grant.

Appendix A. Supporting information

Supplementary data associated with this article can be found in the online version at http://dx.doi.org/10.1016/j.bios.2013.10.068.

References

Bai, L., Chai, Y., Yuan, R., Yuan, Y., Xie, S., Jiang, L., 2013. Biosens. Bioelectron. 50, 325–330.
Bai, Y., Feng, F., Zhao, L., Wang, C., Wang, H., Tian, M., Qin, J., Duan, Y., He, X., 2013. Biosens. Bioelectron. 47, 265–270.
Bard, A.J., Faulkner, L.R., 2000. Electrochemical Methods: Fundamentals and Applications. Wiley, New York.
Bardea, A., Patolsky, F., Dagan, A., Willner, I., 1999. Chem. Commun. 1, 21–22.
Biesecker, G., Dihel, L., Enney, K., Bendele, R.A., 1999. Immunopharmacology 42 (1–3), 219–230.
Blin, F., Koutsoukos, P., Klepetsianis, P., Forsyth, M., 2007. Electrochim. Acta 52 (21), 6212–6220.
Bonanni, A., Esplandiu, M.J., del Valle, M., 2008. Electrochim. Acta 53 (11), 4022–4029.
Bonanni, A., Esplandiu, M.J., del Valle, M., 2010. Biosens. Bioelectron. 26 (4), 1245–1251.
Bonanni, A., Esplandiu, M.J., Pividori, M.I., Alegret, S., del Valle, M., 2006. Anal. Bioanal. Chem. 385 (7), 1195–1201.
Bonanni, A., Pividori, M.I., del Valle, M., 2007. Anal. Bioanal. Chem. 389 (3), 851–861.
Burgering, M.J.M., Orbons, L.P.M., vanderDoelen, A., Mulders, J., Theunissen, H.J.M., Grootenhuis, P.D.J., Bode, W., Huber, R., Stubbs, M.T., 1997. J. Mol. Biol. 269 (3), 395–407.
Cai, H., Wang, Y.Q., He, P.G., Fang, Y.H., 2002. Anal. Chim. Acta 469 (2), 165–172.
Centi, S., Tombelli, S., Minunni, M., Mascini, M., 2007. Anal. Chem. 79 (4), 1466–1473.
Clark, S.L., Remcho, V.T., 2002. Electrophoresis 23 (9), 1335–1340.
Chen, H., Yuan, F., Wang, S., Xu, J., Zhang, Y., Wang, L., 2013. Biosens. Bioelectron. 48, 19–25.
Deng, C., Chen, J., Nie, Z., Wang, M., Chu, X., Chen, X., Xiao, X., Lei, C., Yao, S., 2008. Anal. Chem. 81 (2), 739–745.
Evtugyn, G.A., Kostyleva, V.B., Porfireva, A.V., Savelieva, M.A., Evtugyn, V.G., Sitdikov, R.R., Stoikov, I.I., Antipin, I.S., Hianik, T., 2012. Talanta 102, 156–163.
Fu, H., Ge, C., Cheng, W., Luo, C., Zhang, D., Yan, L., He, Y., Yi, G., 2013. Electroanalysis 25 (5), 1223–1229.
Goda, T., Miyahara, Y., 2013. Biosens. Bioelectron. 45 (1), 89–94.
Gui, G., Zhuo, Y., Chai, Y.Q., Liao, N., Zhao, M., Han, J., Zhu, Q., Yuan, R., Xiang, Y., 2013. Biosens. Bioelectron. 47, 524–529.
Hanaee, H., Ghourchian, H., Ziaee, A.A., 2007. Anal. Biochem. 370 (2), 195–200.
Hicke, B.J., Marion, C., Chang, Y.F., Gould, T., Lynott, C.K., Parma, D., Schmidt, P.G., Warren, S., 2001. J. Biol. Chem. 276 (52), 48644–48654.
Holland, C.A., Henry, A.T., Whinna, H.C., Church, F.C., 2000. FEBS Lett. 484 (2), 87–91.
Jayasena, S.D., 1999. Clin. Chem. 45 (9), 22.
Jenison, R.D., Gill, S.C., Pardi, A., Polisky, B., 1994. Science 263 (5152), 1425–1429.
Katz, E., Willner, I., 2003. Electroanalysis 15 (11), 913–947.
Kong, L., Xu, J., Xu, Y., Xiang, Y., Yuan, R., Chai, Y., 2013. Biosens. Bioelectron. 42 (1), 193–197.
Kotia, R.B., Li, L., McGown, L.B., 2000. Anal. Chem. 72 (4), 827–831.
Lee, M., Walt, D.R., 2000. Anal. Biochem. 282 (1), 142–146.
Lermo, A., Campoy, S., Barbé, J., Hernández, S., Alegret, S., Pividori, M.I., 2007. Biosens. Bioelectron. 22 (9–10), 2010–2017.
Li, Y., Syed, L., Liu, J., Hua, D.H., Li, J., 2012. Anal. Chim. Acta 744, 45–53.
Liao, Y.-M., Feng, Z.-D., Chen, Z.-L., 2007. J. Dent. 35 (5), 425–430.
Lisdat, F., Schafer, D., 2008. Anal. Bioanal. Chem. 391 (5), 1555–1567.
Loo, A.H., Bonanni, A., Ambrosi, A., Poh, H.L., Pumera, M., 2012. Nanoscale 4 (3), 921–925.
McDonald, J.R., 1987. Impedance Spectroscopy. John Wiley, New York.
Merkoci, A., Aldavert, M., Marin, S., Alegret, S., 2005. Trac-Trends Anal. Chem. 24 (4), 341–349.
Ocaña, C., Figueras, C., del Valle, M., 2013. J. Nanosc. Nanotechnol (in press).
Ocaña, C., Pacios, M., del Valle, M., 2012. Sensors 12 (3), 3037–3048.
Pumera, M., Aldavert, M., Mills, C., Merkoci, A., Alegret, S., 2005. Electrochim. Acta 50 (18), 3702–3707.
Radi, A., Acero Sánchez, J.L., Baldrich, E., O'Sullivan, C.K., 2005. Anal. Chem. 77 (19), 6320–6323.
Shi, J., Claussen, J.C., McLamore, E.S., ul Haque, A., Jaroch, D., Diggs, A.R., Calvo-Marzal, P., Rickus, J.L., Porterfield, D.M., 2011. Nanotechnology 22 (35), 355502.
Sivasankar, S., Subramaniam, S., Leckband, D., 1998. Proc. Natl. Acad. Sci. 95 (22), 12961–12966.
Srijanto, B.R., Cheney, C.P., Hedden, D.L., Gehl, A.C., Crilly, P.B., Huestis, M.A., Ferrell, T.L., 2012. Sens. Lett. 10 (3–4), 850–855.
Wang, X.Y., Gao, A., Lu, C.C., He, X.W., Yin, X.B., 2013. Biosens. Bioelectron. 48, 120–125.
Williams, E., Pividori, M.I., Merkoçi, A., Forster, R.J., Alegret, S., 2003. Biosens. Bioelectron. 19 (3), 165–175.
Wu, Z., Liu, Y., Zhou, X., Shen, A., Hu, J., 2013. Biosens. Bioelectron. 44 (1), 10–15.
Xu, H., Gorgy, K., Gondran, C., Le Goff, A., Spinelli, N., Lopez, C., Defrancq, E., Cosnier, S., 2013. Biosens. Bioelectron. 41, 90–95.
Yang, X., Wang, A., Liu, J., 2013. Talanta 114, 5–10.
Zhang, L., Cui, P., Zhang, B., Gao, F., 2013. Chem. Eur. J. 19 (28), 9242–9250.
Zhang, Z., Luo, L., Zhu, L., Ding, Y., Deng, D., Wang, Z., 2013. Analyst 138 (18), 5365–5370.
Zheng, J., Feng, W., Lin, L., Zhang, F., Cheng, G., He, P., Fang, Y., 2007. Biosens. Bioelectron. 23 (3), 341–347.